

INFLUENCE OF IMPELLER'S GEOMETRIC PARAMETERS ON REFRIGERANT FLOW AND THERMAL PERFORMANCE OF A WORKING FLUID PUMP

by

**Huifan ZHENG^{a*}, Yuanqing MA^a, Yongchang WANG^a, Yonggao YIN^b,
Yanjun DAI^c, Xuelai ZHANG^d, and Xin XIN^a**

^a Zhongyuan University of Technology, Zhengzhou, China

^b Southeast University, Nanjing, China

^c Shanghai Jiao Tong University, Shanghai, China

^d Shanghai Maritime University, Shanghai, China

Original scientific paper

<https://doi.org/10.2298/TSCI2004393Z>

In this paper, the refrigerant flow and the thermal performance of a working fluid pump are performed in the perspective of an ejector refrigeration system. The influence of impeller's geometric parameters on the internal pressure, flow rate and cavitation of the pump is studied experimentally and numerically. A vertical multi-stage centrifugal pump is selected as an experimental prototype for numerical verification, and a working fluid pump, which is optimized by the orthogonal analysis, is numerically studied, the results show that the optimized one has better thermal performance than the prototype.

Key words: *working fluid pump, ejector refrigeration, orthogonal analysis, flow performance, thermal performance*

Introduction

With the emphasis on renewable energy worldwide, the solar ejector refrigeration system has received widespread attention in recent years. As the only moving component in the solar ejector refrigeration system, the working fluid pump is particularly important in optimization of the system [1], where the physical characteristics of the refrigerant have a significant influence on the refrigeration properties. Different refrigerants require different pressures during operation, and the special characteristics of the large lift and small flow of the ejector refrigeration system also put forward higher request to the design of the working fluid pump.

There are many parameters influencing the performance of the working fluid pump. The influence of impeller number, diameter and speed on centrifugal pump function were discussed by Abo-Elyamin *et al.* [2] and Jain *et al.* [3] experimentally and numerically. The pressure fluctuation and flow structure of centrifugal pump were studied by Zhang *et al.* [4]. Five impeller models with different blade outlet angles were established by Ding *et al.* [5]. The effects of geometric uncertainty and operational uncertainty on the flow field and performance of low specific speed centrifugal pump were investigated by Salehi *et al.* [6], who concluded that blade geometric uncertainty was the main reason for the velocity change near the blade.

* Corresponding author, e-mail: zhenghuifan@163.com

Some scholars have studied centrifugal pumps used in different systems for transporting special working fluids. Shao *et al.* [7] investigated numerically the effect of different viscous fluids on the unsteady flow of molten salt pump, and revealed the influence of different viscous fluids quantitatively, and the relationship between pump performance and fluid physical characteristics approximately. Deng *et al.* [8] proposed a prediction method for the whole flow performance. Wu *et al.* [9] established a model for organic Rankine cycle by using R245fa as working fluid to analyze and calculate the performance of the system under different working conditions. In addition, other scholars have studied the characteristics of many different types of pumps in working fluid transportation [10-15]. However, there are few studies related to the simulation and experiment of refrigerants under the conditions of the ejector refrigeration system.

The main idea of this study is to find the sequences of factors influencing the efficiency of the working fluid pump, and to carry out an optimal model, which may provide theoretical basis and reference for optimal design of the working fluid pump in future.

Experiment

Multistage centrifugal pump 25CDLF1-36 was selected as the experimental object based on the requirement of ejector refrigeration system for conveying refrigerant. Operation parameters were: designed flow rate, $Q = 1 \text{ m}^3/\text{h}$, head, $H = 200 \text{ m}$, speed, $n = 2900 \text{ rpm}$; geometric parameters of impeller were: impeller diameter was 118 mm, blade outlet width – 3.34 mm, outlet angle – 12.7° , inlet angle – 8.3° , and number of blades – 6.

A working fluid pump test platform was built using multi-stage centrifugal pump as a working fluid pump and R142b as refrigerant. The flow diagram of the working fluid pump test platform was shown in fig. 1, and this platform was composed of a refrigerant cycle and a water cycle. Refrigerant cycle consisted mainly of working fluid pump, heat exchanger, liquid reservoir, sight glass and valves. The water cycle is made up of thermostatic water tank, water pump, heat exchanger and valves.

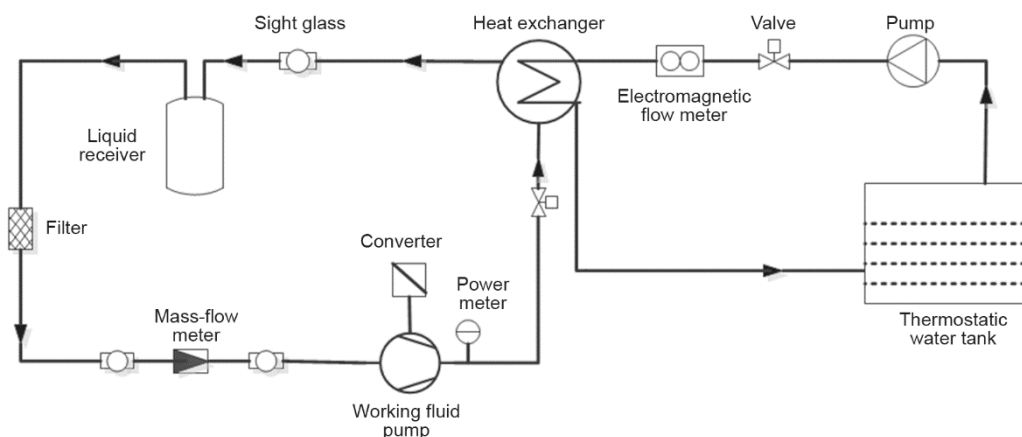


Figure 1. Flow diagram of working fluid pump test platform

At the beginning of the experiment, a certain volume of clean water was added to the thermostatic water tank to stabilize the temperature and pressure of the system. The water side control switch was opened first, and this platform was composed of a refrigerant cycle and a water cycle. Meantime, the flow rate of the pump was adjusted by regulating mass flow-

meter control switch at the outlet of the pump. Under each test condition, the measured values (flow, pressure, etc.) of each test point were recorded at intervals of 10 seconds, and the test time for each test was 10 minutes. The calculated results of experiment were compared with the simulation results in a forthcoming section.

Computational details

Initial design of the model was created by CFturbo. After the initial design was completed, the model was imported into Pumplinx for meshing. Due to the complicated structure of the impeller and the twisted surface of the blade, the Cartesian hexahedron mesh was used to meet the calculation requirement. The impeller grid was shown in fig. 2.

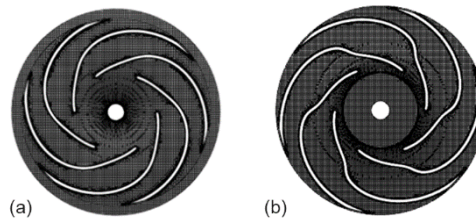


Figure 2. Schematic diagram of impeller grid; (a) first stage, (b) second stage

Assuming that the fluid is incompressible, the mass conservation equation is:

$$\frac{\partial u}{\partial x} + \frac{\partial v}{\partial y} + \frac{\partial \omega}{\partial z} = 0 \quad (1)$$

where u , v and ω constitute velocity vectors in the x -, y - and z -direction, respectively.

Momentum conservation equations are:

$$\frac{\partial(\rho u)}{\partial t} + u \frac{\partial(\rho u)}{\partial x} + v \frac{\partial(\rho u)}{\partial y} + \omega \frac{\partial(\rho u)}{\partial z} = -\frac{\partial p}{\partial x} + \frac{\partial \tau_{xx}}{\partial x} + \frac{\partial \tau_{yx}}{\partial y} + \frac{\partial \tau_{zx}}{\partial z} + \rho f_x \quad (2)$$

$$\frac{\partial(\rho v)}{\partial t} + u \frac{\partial(\rho v)}{\partial x} + v \frac{\partial(\rho v)}{\partial y} + \omega \frac{\partial(\rho v)}{\partial z} = -\frac{\partial p}{\partial y} + \frac{\partial \tau_{xy}}{\partial x} + \frac{\partial \tau_{yy}}{\partial y} + \frac{\partial \tau_{zy}}{\partial z} + \rho f_y \quad (3)$$

$$\frac{\partial(\rho \omega)}{\partial t} + u \frac{\partial(\rho \omega)}{\partial x} + v \frac{\partial(\rho \omega)}{\partial y} + \omega \frac{\partial(\rho \omega)}{\partial z} = -\frac{\partial p}{\partial z} + \frac{\partial \tau_{xz}}{\partial x} + \frac{\partial \tau_{yz}}{\partial y} + \frac{\partial \tau_{zz}}{\partial z} + \rho f_z \quad (4)$$

where ρ is the density, p – the pressure, τ – the viscous force, f_x , f_y , and f_z , – the volume forces in x -, y -, z -directions, respectively.

The energy conservation equation can be expressed:

$$\frac{\partial(\rho T)}{\partial t} + \text{div}(\rho \mu T) = \text{div} \left(\frac{\lambda}{c_p} \text{grad} T \right) + S_T \quad (5)$$

where c_p is the specific heat capacity, λ – the heat transfer coefficient, T – the temperature, S_T – the temperature-related source term. There is no variational formulation for the system of eqs. (1)-(5), the semi-inverse method [16-18] does not work for the present study, so a numerical method has to be adopted in this paper.

Model optimization

Orthogonal analysis

Orthogonal analysis method is used to simulate the selected representative schemes, and the simulation results are analyzed and compared to obtain a better combination in all options. For optimizing the impeller of working fluid pump while keeping the design of inlet

Table 1. Orthogonal table of influencing factors and levels

Factor level	A (blade inlet attack angle)	B (blade outlet angle)	C (blade outlet width)
1	11.7	7.3	2.34
2	12.7	8.3	3.34
3	13.7	9.3	4.34

section and volute unchanged, the main factors affecting pump efficiency are the blade inlet attack angle, blade outlet angle, blade outlet width, blade number, and blade shape in the geometric parameters of impeller. In this research, models with different blade inlet attack angle, blade outlet angle, and blade outlet width are built to study their influence on refrigerant flow and thermal performance of working fluid pump, and an orthogonal factor table is shown in tab. 1.

According to the factors and levels given in tab. 1, different combinations of factors and levels are made, and 27 different combinations are obtained. Nine representative options are selected from all the combinations, and the results are obtained by substituting the selected options into the model calculation as shown in tab. 2.

Table 2. Results of orthogonal analysis

Combination number		Factor		
	1	A1	B1	C1
	2	A1	B2	C3
	3	A1	B3	C2
	4	A2	B1	C3
	5	A2	B2	C2
	6	A2	B3	C1
	7	A3	B3	C1
	8	A3	B2	C2
	9	A3	B1	C3
<i>H</i> [m]	I	546.6	526.5	514.7
	II	539.8	555.7	577.9
	III	553	558	547.7
	<i>k</i> 1	182.2	175.5	171.6
	<i>k</i> 2	179.9	185.2	192.6
	<i>k</i> 3	184.3	186	182.6
	<i>R</i>	3.4	10.5	21
<i>η</i> [%]	I	107.5	108.8	109.4
	II	106.1	104.3	107
	III	107.6	108.1	104.8
	<i>k</i> 1	35.9	36.3	36.5
	<i>k</i> 2	35.4	34.8	35.7
	<i>k</i> 3	35.9	36.0	34.9
	<i>R</i>	0.5	1.5	1.6

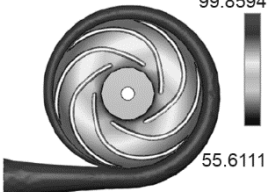
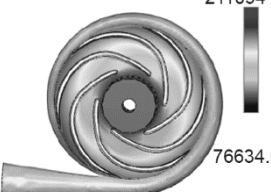

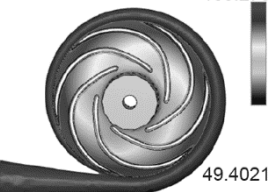
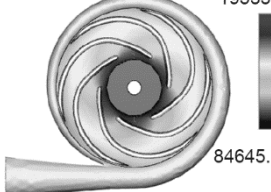

In tab. 2, I, II, and III represent the sum of head or efficiency of numerical simulation corresponding to a factor level in any column, k is the average of I, II, and III. The R is the difference between the maximum and the minimum of k_1 , k_2 , and k_3 in a column.

According to the efficiency of working fluid pump in the orthogonal analysis table, the parameters about efficiency of working fluid pump are blade outlet width, blade outlet angle and blade inlet angle. Through the comparison of nine different schemes, it was found that in the case of low flow, the efficiency of Combination 1 and 6 is higher, reaching 37.6% and 36.3%, respectively. In the case of different flows, Combination 1 has the highest efficiency. However, lift of Combination 6 is higher than that of Combination 1 under the same flow rate. Ultimately, Combination 6 was chosen as the optimal option based on comprehensive consideration.

Results and analysis

The simulation results of prototype and optimization model at rated flow (1 m³/h) are shown in tab. 3. It can be seen that the velocity in the improved model is higher than that of prototype, which means the improved model has better effect on lifting working fluid with the same flow rate. It is shown in the simulation diagram of total pressure distribution that the improved model has more uniform and lower pressure distribution. Therefore, lower local pressure is not easy to cause the local temperature of the fluid in the pump to rise, so that the fluid is uneasy gasified and cause cavitation phenomenon under small flow rate. As for cavitation distribution, cavitation is easy to occur in the central area of the blade root, and the model of prototype has more serious cavitation phenomenon than the improved model.

Table 3. Comparison of simulation results at rated flow

	Velocity distribution	Total pressure distribution	Cavitation distribution
Prototype	Speed of sound [ms ⁻¹] 99.8594  55.6111	Total pressure [Pa] 211094  76634.6	Total gas volume fraction [-] 0.0264575  0.0135215
Improved model	Speed of sound [ms ⁻¹] 105.278  49.4021	Total pressure [Pa] 195339  84645.3	Total gas volume friction [-] 0.0285113  0.0133343

A comparison of the flow and head of the experiment measurement, prototype and optimization model is shown in fig. 3 and 4. By analyzing the curves, it is concluded that the trend of the model results is the same as that of the experimental results. As the flow rate ris-

es, the efficiency curve ascends first and then descends, however, the head curve shows a decreasing trend. At rated flow ($1 \text{ m}^3/\text{h}$), the value of pumping head and efficiency of optimization model are 206.14 m, 35.9%, respectively, and the maximum value are 230.37 m, 37.52%.

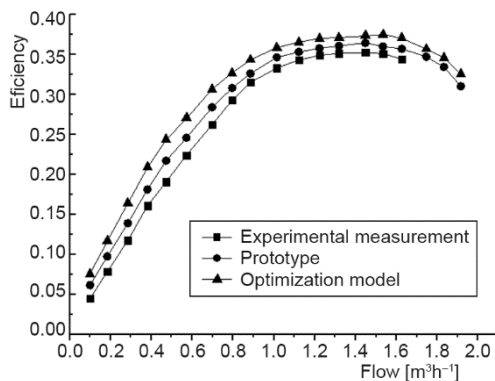


Figure 3. Efficiency comparison chart

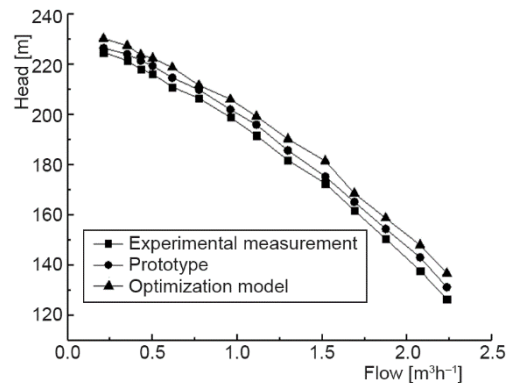


Figure 4. Head comparison chart

Conclusions

The influences of blade outlet width, blade outlet angle and blade inlet angle on refrigerant flow and the thermal performance of the working fluid pump are discussed by using the methods of orthogonal analysis and numerical simulation in this paper. The results show that the improved model is more suitable for ejector-compression system, and the conclusions are summarized as follows.

- According to orthogonal analysis and numerical simulation, an optimal combination of blade outlet width, blade outlet angle, and blade inlet angle is obtained (inlet angle is 12.7° , outlet angle is 9.3° , outlet width is 2.34 mm). The results show that changing the impeller parameters can increase the flow velocity, reduce the pressure at the blade root and reduce cavitation. Meanwhile, the distribution of velocity and pressure in the improved model is more uniform.
- The efficiency curve increases first and then declines when the flow rate rises, and reaches the maximum value 37.52%. With the ascends of flow rate, the curve of head shows a decreasing trend, the maximum value 230.37 m occurs at the minimum flow rate. And when at rated flow, the efficiency is 35.9%, the pumping head is 206.14 m.

Acknowledgment

This work was supported by the Support Plan for Scientific and Technological Innovation Teams in Henan Universities, China (No. 19IRTSTHN010), Key Science and Technology Program of Henan Province, China (No. 202102310550), and also supported by the Scientific Research Foundation of the Higher Education Institutions of Henan Province, China (No. 20A470018).

References

- [1] Besagni, G., et al., Ejector Refrigeration: A Comprehensive Review, *Renewable and Sustainable Energy Reviews*, 53 (2016), 1, pp. 373-407
- [2] Abo-Elyamin, G. R. H., et al., Effect of Impeller Blades Number on the Performance of a Centrifugal Pump, *Alexandria Engineering Journal*, 58 (2019), 1, pp. 39-48

- [3] Jain, S. V., et al., Effects of Impeller Diameter and Rotational Speed on Performance of Pump Running in Turbine Mode, *Energy Conversion and Management*, 89 (2015), 1, pp. 808-824
- [4] Zhang, N., et al., Effects of Modifying the Blade Trailing Edge Profile on Unsteady Pressure Pulsations and Flow Structures in a Centrifugal Pump. *International Journal of Heat and Fluid Flow*, 75 (2019), 1, pp. 227-238
- [5] Ding, H.C. et al., The Influence of Blade Outlet Angle on the Performance of Centrifugal Pump with High Specific Speed, *Vacuum*, 159 (2019), 1, pp. 239-246
- [6] Salehi, S., et al., On the Flow Field and Performance of a Centrifugal Pump Under Operational and Geometrical Uncertainties, *Applied Mathematical Modelling*, 61 (2018), 21, pp. 540-560
- [7] Shao, C. L., et al., Experimental and Numerical Study of External Performance and Internal Flow of a Molten Salt Pump that Transports Fluids with Different Viscosities, *International Journal of Heat and Mass Transfer*, 89 (2015), 9, pp. 627-640
- [8] Deng, H. Y., et al., Whole Flow Field Performance Prediction by Impeller Parameters of Centrifugal Pumps Using Support Vector Regression, *Advances in Engineering Software*, 114 (2017), 12, pp. 258-267
- [9] Wu, T. M., et al., Influence of Working Fluid Pump on System Performance in Organic Rankine Cycle, *Fluid Machinery*, 46 (2018), 2, pp. 68-73
- [10] Peric, M. M., et al., Diesel Production by Fast Pyrolysis of Miscanthus Giganteus, Well-to-pump Analysis Using the Greet Model, *Thermal Science*, 23 (2019), 1, pp. 365-378
- [11] Eames, I. W., et al., An Experimental Investigation into the Integration of a Jet-pump Refrigeration Cycle and a Novel Jet-spray Thermal Ice Storage System, *Applied Thermal Engineering*, 53 (2013), 2, pp. 285-290
- [12] Pereira, P. R., et al., Experimental Results with a Variable Geometry Ejector Using R600a as Working Fluid, *International Journal of Refrigeration*, 46 (2014), 10, pp. 77-85
- [13] Ruangtrakoon, N., Aphornratana, S., Development and Performance of Steam Ejector Refrigeration System Operated in Real Application in Thailand, *International Journal of Refrigeration*, 48 (2014), 12, pp. 142-152
- [14] Zegenhagen, T., Ziegler, F., Experimental Investigation of the Characteristics of a Jet-ejector and a Jet-ejector Cooling System Operating with R134a as a Refrigerant, *International Journal of Refrigeration*, 56 (2015), 8, pp. 173-185
- [15] Thongtip, T., Aphornratana, S., An Alternative Analysis Applied to Investigate the Ejector Performance Used in R141b Jet-pump Refrigeration System, *International Journal of Refrigeration*, 53 (2015), 5, pp. 20-33
- [16] He, J. H., A modified Li-He's Variational Principle for Plasma, *International Journal of Numerical Methods for Heat and Fluid Flow*, On-line first, <https://doi.org/10.1108/HFF-06-2019-0523>, 2019
- [17] He, J. H., Lagrange Crisis and Generalized Variational Principle for 3D unsteady flow, *International Journal of Numerical Methods for Heat and Fluid Flow*, On-line first, <https://doi.org/10.1108/HFF-07-2019-0577>, 2019
- [18] He, J. H., Sun, C., A Variational Principle for a Thin Film Equation, *Journal of Mathematical Chemistry*, 57 (2019), 9, pp. 2075-2081